Journal of Nuclear Materials 385 (2009) 262–267

Contents lists available at ScienceDirect

Journal of Nuclear Materials

journal homepage: www.elsevier.com/locate/jnucmat

Multiscale modelling of bi-crystal grain boundaries in bcc iron

Ning Gao [a], Chu-Chun Fu [b], M. Samaras [a,*], R. Schäublin [c], M. Victoria [a,d,e], W. Hoffelner [a]

[a] Laboratory for Nuclear Materials, NES, Paul Scherrer Institute, Switzerland
[b] SRMP, CEA/Sarclay, 91191 Gif Sur Yvette, France
[c] Ecole Polytechnique Fédérale de Lausanne (EPFL), Center for Research in Plasma Physics, Association Euratom-Confédération Suisse, Switzerland
[d] Lawrence Livermore National Laboratory, Chemistry and Materials Science, Livermore, CA 94550, USA
[e] Polytechnic University of Madrid, Institute of Nuclear Fusion, 28006 Madrid, Spain

ARTICLE INFO

PACS:
83.10.Rs
61.72.Mm
68.35.−p

ABSTRACT

Atomistic simulations have provided much insight into grain boundary (GB) structures and mechanisms which are important in understanding the properties of materials. In this paper, the $\sum 3\{1\,1\,2\}$, $\sum 3\{1\,1\,1\}$ and $\sum 5\{0\,1\,3\}$ (coincidence site lattice) GBs of bcc iron are investigated using molecular statics (MS) simulations, *ab initio* DFT calculations and the simulated HRTEM method. For the MS calculations, four empirical potentials, the Ackland potential (1997), Mendelev potentials 2 and 4 and the Dudarev–Derlet potential have been used. The MS results for all three symmetrical grain boundaries show the results to be independent of the empirical potential implemented. After relaxation, the symmetrical structures of the GBs remain, in agreement with *ab initio* calculation results.

1. Introduction

A large number of materials of technological use are composed of polycrystals. Grain boundaries (GBs) play an important role in crystalline materials as they control many of the material's physical and chemical properties [1,2]. At high temperature and during irradiation, GBs act as sinks or sources for interstitials and vacancies. In nuclear applications, diffusion of such defects in GBs is of great interest. Understanding how atoms move to and within GBs enables the study of voids [3] and/or bubble nucleation at GBs, whose fast accumulation leads to cracks and is important in comprehending the creep lifetime expectancy of metals. To investigate the role of the GB, it is first necessary to deduce which GB configurations are stable. In cubic materials periodic GB structures are often observed. The coincidence site lattice (CSL) concept can therefore be used to create samples containing GBs. This geometrical concept stems from the idea that a high density of coincidence sites are present in low energy GBs. Using the CSL method, computer simulated samples can be generated to study GBs at an atomistic level. In recent years, atomistic simulation studies of GBs have been performed using molecular statics (MS), molecular dynamics (MD) and *ab initio* calculations.

The simplicity of the $\sum 3\{1\,1\,2\}$ GB in bcc metals has lead to its study for over 40 years. This GB has mirror symmetrical tilt configuration with a rotation angle of 70.53°. Various atomistic modelling has been conducted using a variety of potentials, from pair potential of Johnson [4] and Beauchamp [5] to tight-binding [6] and many-body potentials, such as Finnis-Sinclair type potentials [7–9]. A multiscale approach [10] modelling bcc Mo and Nb, using *ab initio* and semi-empirical methods, two final states for the $\sum 3\{1\,1\,2\}$ GB were found, a 'refection state' and a 'sheared state', depending on the empirical potential or *ab initio* method used. In the case of the $\sum 3\{1\,1\,1\}$ GB, whose rotation angle is 109.47°, simulations of sliding and decohesion at the GB with pairwise interatomicpotential and *ab initio* many-body potentials performed for bcc W indicate that the mirror symmetrical configuration is stable [11]. The $\sum 5\{0\,1\,3\}$ GB is yet another bcc metal bi-crystal structure that has been studied using six different theoretical total-energy schemes for Mo and Nb [12]. In that study, most schemes predict a 'reflection state' with fully or nearly conserved mirror symmetry for Nb, whereas a 'sheared state' with broken mirror symmetry was found for Mo. From the point of view of experiment, it is not very easy to prepare the samples for symmetrical grain boundaries of bcc iron and to the magnetism present makes HRTEM difficult to perform, therefore, until now there have not been many papers reporting on GBs of bcc iron.

In the present paper, the energies and configurations of three tilt symmetrical GBs, the $\sum 3\{1\,1\,2\}$, $\sum 3\{1\,1\,1\}$ and $\sum 5\{0\,1\,3\}$ GBs of bcc iron are investigated using a synergistic multiscale modelling scheme comparing first principle *ab initio* calculations and four different empirical many-body potential simulations, to investigate the stable configuration for each GB structure. The next section outlines the simulation techniques used as well as the construction of the GBs; then the results obtained are discussed and the final section concludes the paper.

* Corresponding author. Tel.: +41 56 310 4184; fax: +41 56 310 4595.
E-mail address: maria.samaras@psi.ch (M. Samaras).

0022-3115/$ - see front matter © 2008 Elsevier B.V. All rights reserved.
doi:10.1016/j.jnucmat.2008.12.016

2. Method

Atomistic calculations have been performed with supercells containing two grains of bcc Fe with periodic boundary conditions imposed. In a multiscale effort, *ab initio* results are compared to empirical potential molecular statics (MS) calculations. A two tier system is used, where the potentials are implemented at 0 K in the MS calculations and compared to *ab initio* results. The GB structures investigated are the $\sum 3\{1\,1\,2\}$, $\sum 3\{1\,1\,1\}$ and $\sum 5\{0\,1\,3\}$ GBs of bcc iron.

The results of reference *ab initio* calculations have been performed in the framework of the density functional theory in the generalized gradient approximation (DFT-GGA) using the SIESTA (Spanish initiative for electronic simulations with thousands of atoms) code. The SIESTA DFT-GGA method provides an accuracy comparable to that of more robust planewave codes, but with significantly less computational efforts [13] which makes it possible to simulate extended defects such as GBs. The simulation cells contain from 192 to 240 atoms. The Methfessel-Paxton broadening scheme is used with a 0.3 eV width and $4 \times 4 \times 1$ *k*-point grids for $\sum 3\{1\,1\,2\}$ and $\sum 5\{0\,1\,3\}$ GBs, and $4 \times 3 \times 2$ for $\sum 3\{1\,1\,1\}$. The resulting GB formation energies have been checked to be well converged, their variations remain smaller than 1% with further increase of *k*-point grids.

In the MS simulations, for $\sum 3\{1\,1\,2\}$ and $\sum 3\{1\,1\,1\}$, the three directions are set as follows: $x[1\,1\,0]$, $y[1\,\bar{1}\,1]$ and $z[\bar{1}\,1\,2]$. The number of unit cells for these two grain boundaries along *x*, *y* and *z* direction are $20 \times 20 \times 20$. For the $\sum 5\{0\,1\,3\}$ GB, the *x*, *y* and *z* directions are chosen as: $x[0\,0\,1]$, $y[3\,1\,0]$ and $z[\bar{1}\,3\,0]$. The number of unit cells along each direction in the MS simulations are $15 \times 12 \times 12$. The distance between these two GBs is determined by the number of layers between them. For convenience, the number of layers are defined as follows: the GB as the 0 layer, the nearest layer from the upper/lower grain as +1/−1 layer, the second nearest layer from the upper/lower grain as +2/−2 layer and so on.

MS simulations have been performed to relax the pure Fe bicrystal samples to determine the energetics of the specific GBs. During the simulation, the structures were optimized by relaxing the atomic positions, volume and shape of the computational supercells using the Parrinello–Rahman algorithm [14]. Four empirical potentials were used to perform the MS simulations, the Ackland [15], Mendelev 2 [16], Mendelev 4 [16] and Dudarev–Derlet (DD) [17] potentials. The Ackland potential has been refitted and the results calculated with these new parameters

Table 1
Grain boundary energies of $\sum 3\{1\,1\,2\}$, $\sum 3\{1\,1\,1\}$ and $\sum 5\{0\,1\,3\}$ of bcc iron calculated with MS and *ab initio* simulations. The units for these results are J/m^2.

	Ackland (1997)	Mendelev (2)	Mendelev (4)	DD potential	*Ab initio*	Other MD results	Ref.
$\sum 3\{1\,1\,2\}$	0.3871	0.3220	0.3104	0.3233	0.3400	0.3000 0.2700	[22,23]
$\sum 3\{1\,1\,1\}$	1.5466	1.2978	1.2194	1.3852	1.5200	1.2300	[23]
$\sum 5\{0\,1\,3\}$	1.2582	0.9869	1.0155	1.2992	1.4888	1.1090	[24]

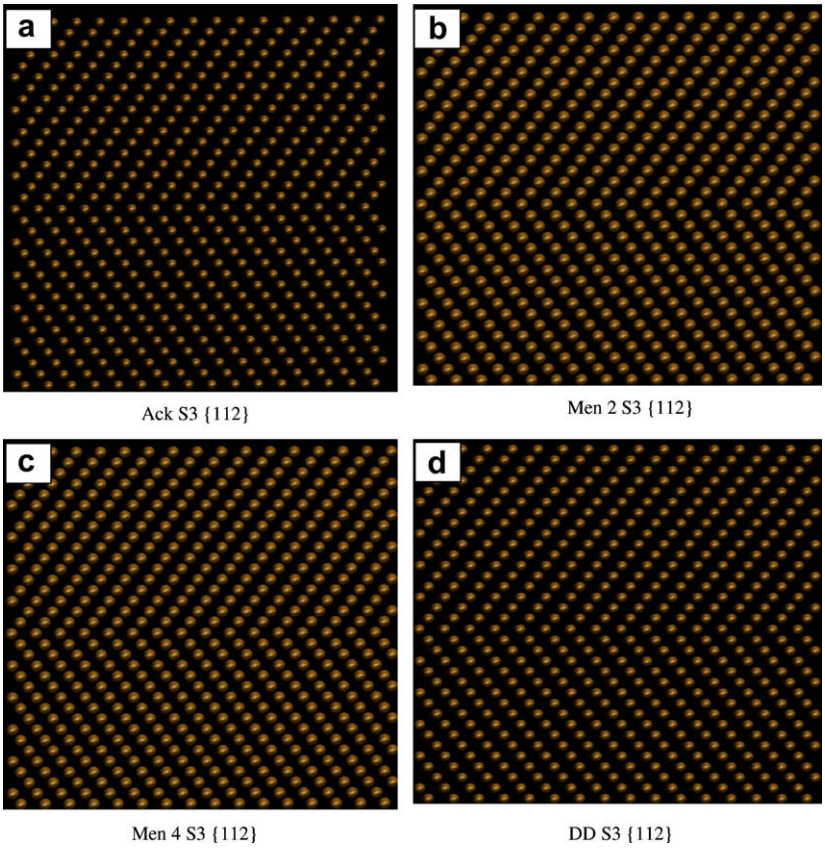

Fig. 1. (a)-(d) Relaxed configurations of $\sum 3\{1\,1\,2\}$ obtained from four different empirical potentials, (a) Ackland potential, (b) and (c) Mendelev potential 2 and 4, (d) DD potential.

show a good agreement with *ab initio* results. Main differences in the potentials are as follows: in the Ackland potential, the crowdion and the <1 1 0> dumbbell are almost degenerate interstitial configurations which contradicts experimental evidence and *ab initio* calculations. The Mendelev potential has corrected this, such that the <1 1 0> dumbbell is the most stable interstitial configuration. The DD potential, with correct interstitial stability, is the only potential which includes the effect of magnetism. The cutoff distance of these four potentials varies between 3.76 and 6.00 Å. The Ackland potential has the shortest cutoff distance. The cutoff distance of the DD potential is 4.1 Å. The Mendelev potential 2 has a cutoff distance 5.3 Å and potential 4 is 6.0 Å. For each configuration the samples were relaxed for 60 ps. The MS samples investigated contain between 2400 and 50,000 atoms. The different sample sizes have been investigated in order to check for size effects.

The GB formation energy, $\gamma_{gb,}$ is defined as the difference between the potential energy E_{gb} of n atoms in the supercell containing GBs and the potential energy E_p^o of a computational cell with the same number of atoms in a perfect crystal, divided by the cross-sectional area, S, of the GB plane. Note: in these simulations two GBs exist in the supercells due to periodic boundary conditions,

$$\gamma_{gb} = \frac{E_{gb} - E_p^o}{2s}. \quad (1)$$

The energy of the perfect lattice is calculated with all four potentials. The perfect lattice is set in a direction similar to that of the bi-crystal samples. For the different potentials used in MS, the cohesive energy per atom of bcc iron was calculated in advance and compared with the original value provided by other authors. The perfect lattice potential energies from these four potentials are: −4.3160 eV (c.f. −4.316 eV [15]) for Ackland potential, −4.1224 eV (c.f. −4.122 eV [16]) for Mendelev potential 2, −4.1554 eV (c.f. −4.155 eV [16]) for Mendelev potential 4 and −4.3160 eV (c.f. −4.316 eV [17]) for DD potential. For consistency, these results are used as the potential energy of perfect crystal.

Transmission electron microscopy is a useful technique to investigate GBs. With either HRTEM, based on phase contrast, or conventional TEM, based on diffraction contrast [18,19], one can have access to the rigid lattice displacement induced by a GB. TEM image simulations performed here are based on the multislice technique [20] whereby all sample atoms, which scatter the electron wave, are considered. The simulations are performed with the code described in Kirkland [21]. Images were done with 200 kV, a spherical aberration of 1 mm, an aperture of 60 mrad and at Scherzer defocus (613.3 Å).

3. Results

The GB energies of $\sum 3\{1\,1\,2\}$, $\sum 3\{1\,1\,1\}$ and $\sum 5\{0\,1\,3\}$ of bcc iron calculated with MS and *ab initio* simulations are listed in Table 1. The final column of Table 1 includes the results of other authors performing MD simulations on bcc Fe [22–24]. The Ackland potential, F-S and EAM potentials are used in reference 22 to 24, respectively. In Table 1, the *ab initio* calculations are performed on samples containing 192 atoms and the results of the MS calculations contain approximately 50,000 atoms. The results from smaller computational supercells have also been calculated in order to

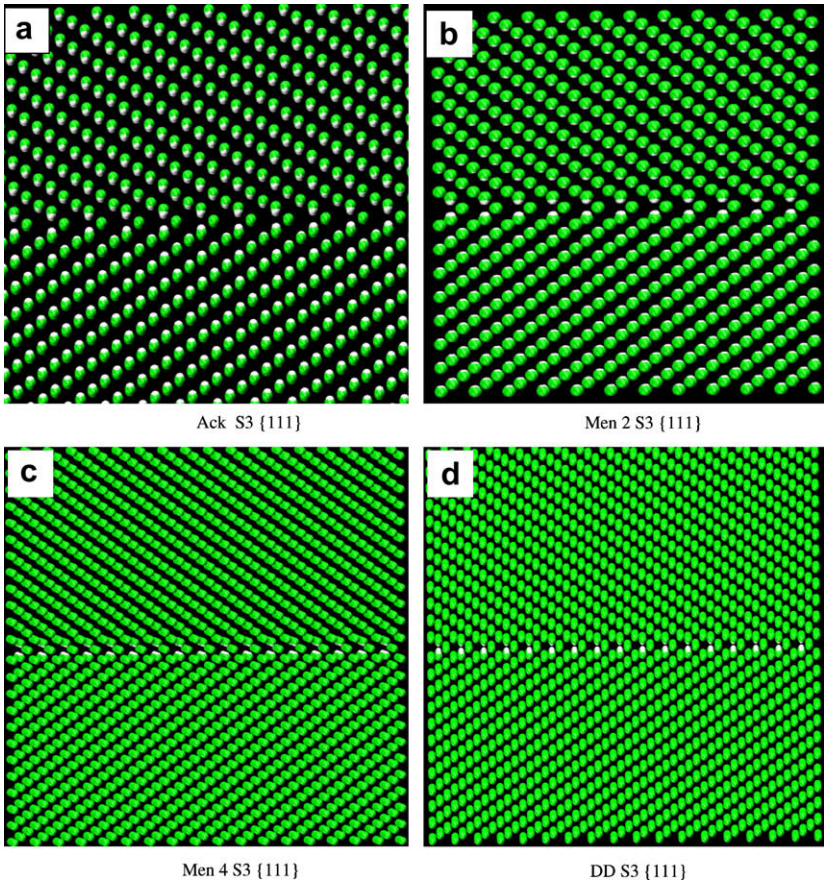

Fig. 2. (a)-(d) Relaxed and unrelaxed configurations of $\sum 3\{1\,1\,1\}$ obtained from four different empirical potentials, (a) Ackland potential, (b) and (c) from Mendelev potential 2 and 4, (d) from DD potential. Unrelaxed and relaxed configurations are represented by green and grey spheres, respectively. (For interpretation of the references to colour in this figure legend, the reader is referred to the web version of this article).

investigate possible size effects, but are omitted as these results are very close to those of the larger supercell results. For $\sum 3\{1\,1\,2\}$, the results from the refitted Ackland and DD potentials are closer to the *ab initio* results than the Mendelev potential 2 and 4 results. For $\sum 3\{1\,1\,1\}$, the values from the refitted Ackland potential is closest to the *ab initio* result. For $\sum 5\{0\,1\,3\}$, the refitted Ackland and DD potentials results are closest. Table 1 also includes results of other authors who have performed MD simulations [22–24]; these results differ to our results. This is due to the use of other potentials or in the case where the same potentials is used, it could be a temperature effect as the MD simulations are performed at a non-zero temperature, whereas our simulations are performed at 0 K in both MS and *ab initio* calculations, or due to the use of different boundary conditions [25], and/or different criteria of geometry optimization such as force and stress tolerance.

To explain why such differences in energies occur from the different empirical potentials used, the GBs are visualized in Figs. 1 and 2. For $\sum 3\{1\,1\,2\}$, the structure do not change greatly along the direction parallel to GB plane or perpendicular to GB plane, therefore in Fig. 1, only the relaxed structures are shown. In these simulations, approximately 50,000 atoms are used with periodic boundary condition. The figures show a small section of the simulation cell near the GB. The geometrical configurations for $\sum 3\{1\,1\,2\}$ are shown in Fig. 1(a)–(d), where Fig. 1(a) is the result from the refitted Ackland potential, Fig. 1(b) and (c) from Mendelev potentials 2 and 4, and Fig. 1(d) from the DD potential. From Fig. 1, it is clear that the final fully relaxed configurations calculated with these four potentials are similar. The original symmetrical structures have not been broken. The atoms at the GB in the direction perpendicular to GB plane in the relaxed structure have been displaced. The displacement vector is very small compared to the original positions. That means the lowest energy of this grain boundary is a 'reflected state' and the stress filed near the grain boundary is not very big. The *ab initio* results show a 'reflected state' with no appreciable movement in this GB. Thus the *ab initio* results confirm the MS results obtained by all four empirical potentials. For the $\sum 3\{1\,1\,2\}$ GB of bcc iron, the energy and configurations indicate that it is a stable GB and can be used as a reference GB to perform further research using empirical potentials. This differs to the conclusion for bcc Mo and Nb, where the $\sum 3\{1\,1\,2\}$ GB was found to be unstable and cannot be used as a reference GB [26].

It is important to emphasise this result is only valid for $\sum 3\{1\,1\,2\}$ GBs in bcc Fe. This reflected state is also seen in conventional TEM pictures of $\sum 3\{1\,1\,2\}$ Fe GBs [18]. From that experiment, Forwood et al. reported the configuration of $\sum 3\{1\,1\,2\}$ GBs in bcc Fe are symmetrical boundaries. Although HRTEM would provide higher spatial resolution, HRTEM of Fe is scarce due to the magnetic effect which disturbs the electron optics, and image interpretation is less straightforward, as the image presents a strong dependence on defocus and specimen thickness. The structure of the specimen can therefore not be deduced in a straightforward manner from the image, also because the image records the intensity of the electron wave, not its amplitude and phase [27]. Hence, whether or not the small displacements of atoms near the GB, are visible using experimental HRTEM is questionable. One possible methodology to bridge the gap is to simulate HRTEM images [28] of the model GBs and compare the final structures with those seen in experiment. Such type of work has enabled the visualisation of small lattice displacements at GBs [29]. HRTEM images of the $\sum 3\{1\,1\,2\}$ relaxed samples have been simulated and are shown in Fig. 3(a)–(d) for the refitted Ackland, Mendelev 2, Mendelev 4 and DD potentials, respectively. For the Ackland and DD potentials, the symmetrical structure has remained. These predicted structures are agreement with experimental results [18]. For the Mendelev 2 and 4 potentials, the shift present in these samples is very small and not clearly visible. This has a few implications: it will be necessary to perform more intensive image simulations to try and resolve the shift present, and more importantly it indicates the necessity to use first principle calculations to check which

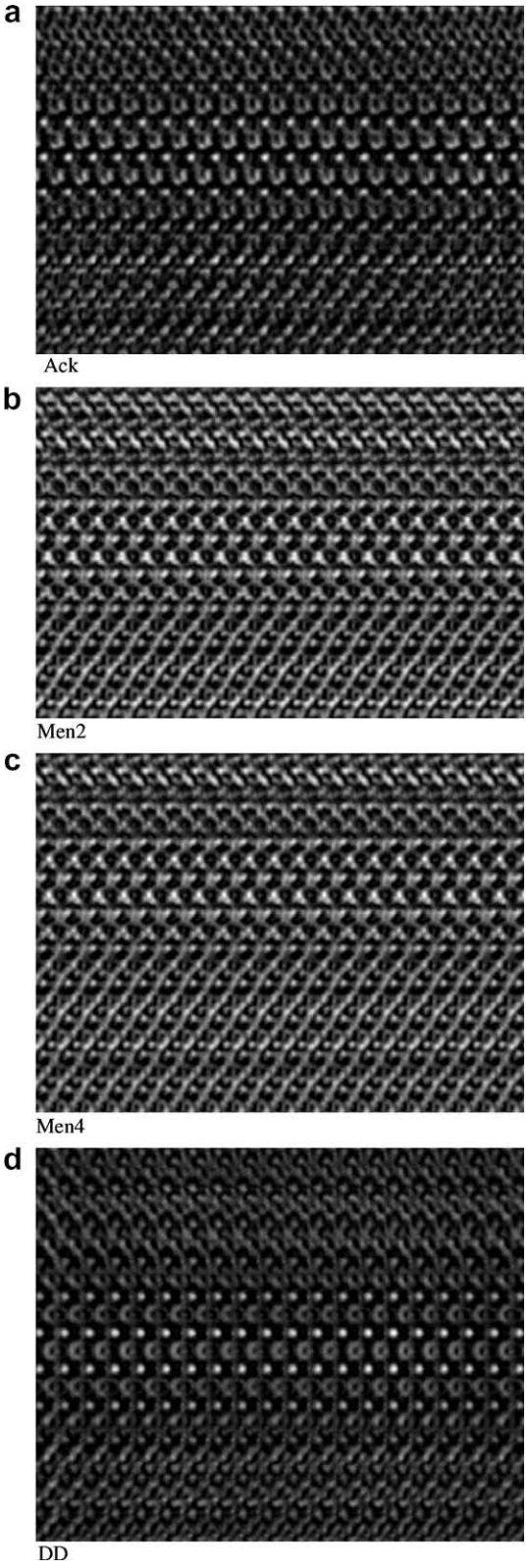

Fig. 3. (a)-(d) HRTEM simulations of the relaxed configurations of $\sum 3\{1\,1\,2\}$ (those of Fig. 1) of the four different empirical potentials, (a) Ackland potential, (b) and (c) from Mendelev potential 2 and 4, and (d) from DD potential.

potential best reproduces the GB structure in order to perform MD simulations.

The $\sum 3\{1\,1\,1\}$ GB of bcc iron calculated, whose geometrical structures of unrelaxed and relaxed GB configurations, using the four empirical potentials (refitted Ackland, Mendelev 2, Mendelev 4, DD potential), are shown in Fig. 2(a)–(d), respectively. In this GB, the figures show that the mirror symmetrical configurations of the relaxed system have not been broken by any of the potentials. However, the relative distance between two reflected layers has changed. The maximal change in relative distance is at the two closest layers (+1/−1 layers) to the GB. From Fig. 2, it is clear to see that the empirical potentials show a similar movement for atoms perpendicular to GB. The distance between atoms at the $+n$ and $-n$ layers increases, from 0.2599 to 0.696 Å. The further from the GB plane, the less the movement of the atoms. To understand this phenomenon, research could be performed on the stress field near the GB.

The change of interlayer distance for the $\sum 3\{1\,1\,2\}$ and $\sum 3\{1\,1\,1\}$ GBs before and after full relaxation are calculated with all four potentials and is shown in Fig. 4. Although MS generated samples contain many more layers, only the first 11 layers are shown in order to make a comparison to the *ab initio* calculations as shown in Fig. 5. For $\sum 3\{1\,1\,2\}$, the results from the four potentials are similar. The change is very small for layers near the GB, and from the 4th layer, the change of interlayer distance is close to zero and can be neglected. A similar result is found with the *ab initio* calculations where the 13th layer is the position of the second GB in the sample. These results indicate that the stress field of the $\sum 3\{1\,1\,2\}$ GB is not long-ranged. The results from these four empirical potentials are close to results from the *ab initio* calculations.

For the $\sum 3\{1\,1\,1\}$ GB the difference is larger than that of $\sum 3\{1\,1\,2\}$. The movement of the atoms from the unrelaxed position oscillates between positive and negative. From Figs. 4 and 5, it can be seen that the results from all four potentials are similar to those of the *ab initio* calculations. The results from *ab initio* show that the change in distance between the GB and the first nearest layer (D_1) is very close to the change between the first and second layer (D_2), and these two changes are the maximal values amongst the movement of atoms at different layers. Results of the four potentials differ slightly. These results show that for the $\sum 3\{1\,1\,1\}$ GB, empirical potential completely captures the trends seen in the *ab initio* results.

The results of the $\sum 3$ GB show that by using only an empirical potential, one can obtain similar results to *ab initio* calculations. However, for other bcc metals, the 'reflected' or 'sheared' structures may be the state with the lowest energy. Indeed, every method has its limits and when the difference between two structures is below this limit, it is not possible to say which structure is the more stable [10]. For this reason it is important to compare results to more precise *ab initio* calculations and to experiment, to help choose which empirical potentials are appropriate to implemented in larger scale simulations. From our simulations, we see that empirical potentials can be used to simulate bcc Fe GBs. However, further research for the lowest energy state of $\sum 3$ GB is still needed with new better methods.

For the $\sum 5\{0\,1\,3\}$ GB, the relaxed configurations using all four potentials are all very similar. The mirror symmetrical configurations have not been broken and the relative distance between reflected layers has also not changed greatly. This means that the configuration has not changed and therefore is not shown. Like $\sum 3\{1\,1\,2\}$ and $\sum 3\{1\,1\,1\}$, the results for the $\sum 5\{0\,1\,3\}$ GB are not dependent on the empirical potential used. According to these results, since the $\sum 5\{0\,1\,3\}$ GB is potential independent, it is a good GB to use for benchmarking phenomena in bi-crystal when performing MD or MS calculations. It is important to note that the results for these GB are only relevant for bcc iron, not for other bcc metals such as Mo [12] where symmetry breaking in $\sum 5\{0\,1\,3\}$ was seen.

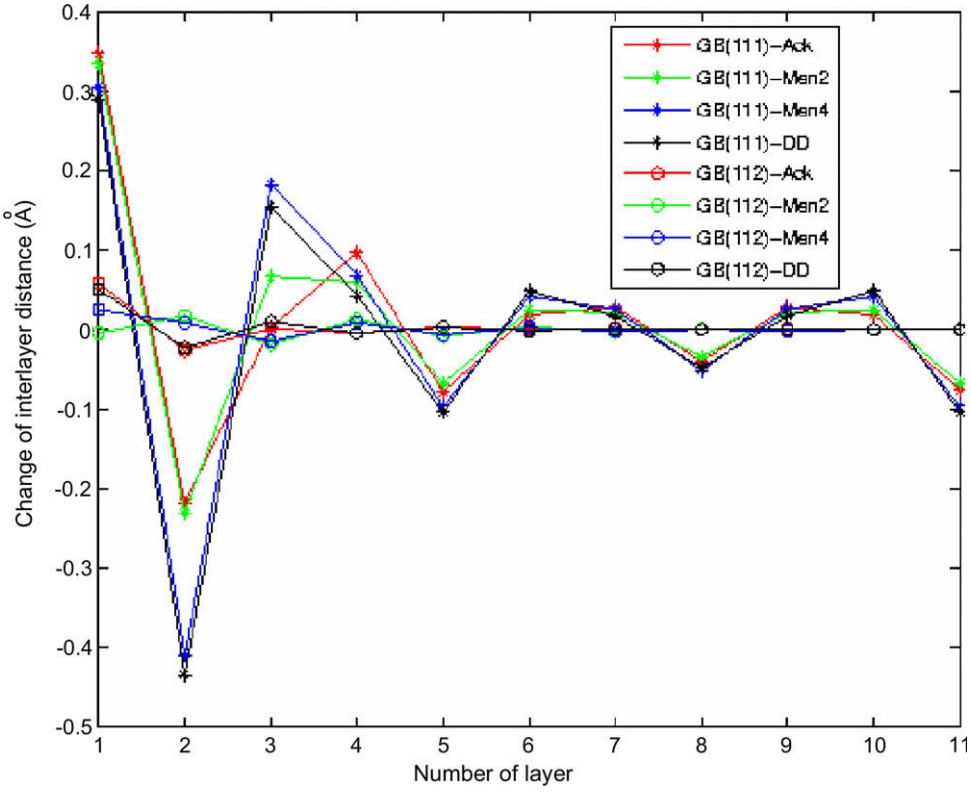

Fig. 4. Changes of interlayer distances calculated with four empirical potentials after full relaxations with respective original unrelaxed distances for $\sum 3\{1\,1\,2\}$ and $\sum 3\{1\,1\,1\}$.

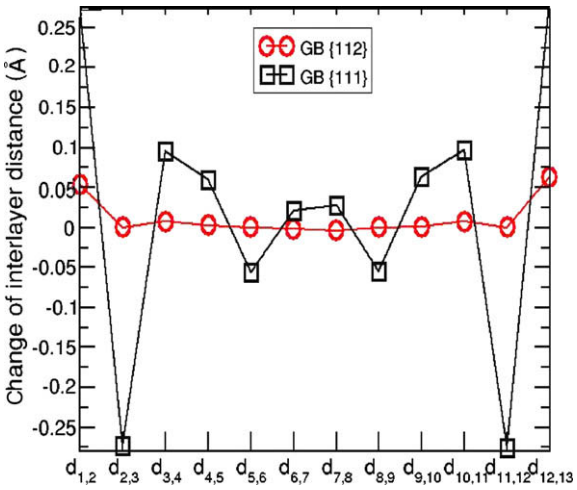

Fig. 5. Changes of interlayer distances calculated with *ab initio* after full relaxations with respective original unrelaxed distances for $\sum 3\{112\}$ and $\sum 3\{111\}$.

Table 2
Excess volumes of the different grain boundaries using different empirical potentials in MS simulations.

	Ackland (1997)	Mendelev 2	Mendelev 4	DD potential
$\sum 3\{112\}$	1.0008	0.9999	1.0003	1.0005
$\sum 3\{111\}$	1.0279	1.0256	1.0131	1.0062
$\sum 5\{013\}$	1.0048	1.0064	1.0046	1.0033

Another calculation performed was an excess ratio volume estimation, recorded in Table 2, which results as a consequence of the introduction of the GB. In these calculations, relaxations were performed for atomic positions, volume and shape of the computational box. The excess ratio volume is defined as the volume of the bi-crystal computational box after relaxation divided by the volume of the single crystal sample containing the same number of atoms. From Tables 1 and 2, it is easy to see that the GB energy increases linearly with the change in excess volume. It is also interesting to note that (1) the difference in excess volume calculated with the DD potential for the various GBs is not appreciable. A possible reason could be attributed to the magnetic effect included in the DD potential. (2) The GB energy for $\sum 5\{013\}$ is much larger than that of $\sum 3\{112\}$. The variation in excess ratio volume of these two GBs, however, is quite close, unlike the difference between $\sum 3\{112\}$ and $\sum 3\{111\}$. This indicates that the GB energy is not only related to the excess volume but also with other effects. To understand these changes further first principle calculations of the electronic density would be necessary.

4. Conclusion

Multiscale atomistic simulations using *ab initio* SIESTA and empirical potential molecular statics simulations have been performed on bi-crystal bcc iron samples containing a $\sum 3\{112\}$, $\sum 3\{111\}$ or $\sum 5\{013\}$ grain boundary (GB). For all GBs, the $\sum 3\{112\}$, $\sum 3\{111\}$ and $\sum 5\{013\}$, MS results indicate that the emprical potentials, Ackland, Mendelev 2 and 4, and Dudarev–Derlet, deliver results very similar to *ab initio* calculations. Results obtained are independent of the potential used. The lowest energy states for these three grain boundaries are 'reflected' structures. The TEM simulations also show the symmetrical state. These results indicates the importance of using a multiscale modelling technique with a first principle formalism to check if the relaxed configurations of GBs of the particular material under investigation are correct in larger scale models before proceeding further in the investigation of their properties.

References

[1] C.C. Koch, D.G. Morris, K. Lu, A. Inoue, MRS Bulletin 24 (1999) 54.
[2] A.P. Sutton, R.W. Balluffi, Interfaces in Crystalline Materials, Clarendon, New York, 2005.
[3] M. Samaras, W. Hoffelner, M. Victoria, J. Nucl. Mater. 352 (2006) 50.
[4] R.A. Johnson, Phys. Rev. A 134 (1964) 1329.
[5] P. Beauchamp, Phil. Mag. A 37 (1978) (167 and 179).
[6] A.M. Papon, J.P. Simon, P. Guyot, M.C. Desjonqueres, Phil. Mag. B 40 (1979) 159.
[7] A.G. Marinopoulos, V. Vitek, A.E. Carlsson, Phil. Mag. A 72 (1995) 1311.
[8] M.W. Finnis, J.E. Sinclair, Phil. Mag. A 50 (1984) 45.
[9] G.J. Ackland, R. Thetford, Phil. Mag. A 56 (1987) 15.
[10] M. Mrovec, T. Ochs, C. Elsasser, V. Vitek, D. Nguyen-Manh, D.G. Pettifor, Z. Metallkd. 94 (2003) 3.
[11] S. Dorfman, D.E. Ellis, K.C. Mundim, V. Liubich, D. Fuks, Adv. Eng. Mater. 4 (2002) 580.
[12] T. Ochs, C. Elsesser, M. Mrovec, J. Belak, J.A. Moriarty, Phil. Mag. A 80 (2000) 2405.
[13] C.C. Fu, F. Willaime, P. Ordejon, Phys. Rev. Lett. 92 (2004) 175503.
[14] M. Parrinello, A. Rahman, J. Appl. Phys. 52 (1981) 7182.
[15] G.J. Ackland, D.J. Bacon, A.F. Calder, T. Harry, Phil. Mag. A 75 (1997) 713.
[16] M.I. Mendelev, S. Han, D.J. Srolovitz, G.J. Ackland, D.Y. Sun, M. Asta, Phil. Mag. 83 (2003) 3977.
[17] S.L. Dudarev, P.M. Derlet, J. Phys. Condens. Mat. 17 (2005) 7097.
[18] C.T. Forwood, L.M. Clarebrough, Phys. Stat. Sol. (a) 105 (1988) 365.
[19] R. Schäublin, P. de Almeida, A. Almazouzi, M. Victoria, J. Nucl. Mater. 283&287 (2005) 205.
[20] J.M. Cowley, A.F. Moodie, Acta Crystallogr. 10 (1957) 609.
[21] E.J. Kirkland, Advanced Computing in Electron Microscopy, Plenum Publishing Company, New York, 1998.
[22] F. Gao, H. Heinisch, R.J. Kurtz, J. Nucl. Mater. 351 (2006) 133.
[23] H. Nakashima, M. Takeuchi, Iron Steel Inst. Japan (ISIJ) 86 (2000) 357.
[24] B. Hyde, Effects of Carbon on Fracture Mechanisms in Nanocrystalline BCC Iron-Atomic Simulations, PhD thesis, Virginia Polytechnic Institute and State University, 2004.
[25] R.J. Kurtz, H.L. Heinisch, J. Nucl. Mater. 1199 (2004) 329.
[26] V. Vitek, Scripta Metall. 4 (1970) 725.
[27] F. Ernst, D. Hofmann, K. Nadarzinski, C. Schmidt, S. Stemmer, S.K. Streiffer, Mater. Sci. Forum 23 (1996) 207.
[28] R. Schäublin, P. de Almeida, A. Almazouzi, M. Victoria, J. Nucl. Mater. 205 (2005) 283.
[29] C.Y. Chen, R. Schäublin, W.M. Stobbs, Mater. Sci. Eng. A360 (2003) 356.